Dartmouth College

# Dartmouth Digital Commons

Open Dartmouth: Peer-reviewed articles by Dartmouth faculty

Faculty Work

2-1997

# C-terminal Truncations of the Yeast Nucleoporin Nup145p Produce a Rapid Temperature-conditional mRNA Export Defect and Alterations to Nuclear Structure.

Thomas C. Dockendorff
*Dartmouth College*

Catherine V. Heath
*Dartmouth College*

Alan L. Goldstein
*Dartmouth College*

Christine A. Snay
*Dartmouth College*

C N. Cole
*Dartmouth College*

Follow this and additional works at: https://digitalcommons.dartmouth.edu/facoa

Part of the Medical Biochemistry Commons, Medical Cell Biology Commons, and the Medical Molecular Biology Commons

# C-Terminal Truncations of the Yeast Nucleoporin Nup145p Produce a Rapid Temperature-Conditional mRNA Export Defect and Alterations to Nuclear Structure

THOMAS C. DOCKENDORFF,† CATHERINE V. HEATH, ALAN L. GOLDSTEIN,‡
CHRISTINE A. SNAY, AND CHARLES N. COLE*

*Department of Biochemistry, Dartmouth Medical School, Hanover, New Hampshire 03755*

A screen for temperature-sensitive mutants of *Saccharomyces cerevisiae* defective in nucleocytoplasmic trafficking of poly(A)$^+$ RNA has identified an allele of the *NUP145* gene, which encodes an essential nucleoporin. *NUP145* was previously identified by using a genetic synthetic lethal screen (E. Fabre, W. C. Boelens, C. Wimmer, I. W. Mattaj, and E. C. Hurt, Cell 78:275–289, 1994) and by using a monoclonal antibody which recognizes the GLFG family of vertebrate and yeast nucleoporins (S. R. Wente and G. Blobel, J. Cell Biol. 125:955–969, 1994). Cells carrying the new allele, *nup145-10*, grew at 23 and 30°C but were unable to grow at 37°C. Many cells displayed a modest accumulation of poly(A)$^+$ RNA under permissive growth conditions, and all cells showed dramatic and rapid nuclear accumulation of poly(A)$^+$ RNA following a shift to 37°C. The mutant allele contains a nonsense codon which truncates the 1,317-amino-acid protein to 698 amino acids. This prompted us to examine the role of the carboxyl half of Nup145p. Several additional alleles that encode C-terminally truncated proteins or proteins containing internal deletions of portions of the carboxyl half of Nup145p were constructed. Analysis of these mutants indicates that some sequences between amino acids 698 and 1095 are essential for RNA export and for growth at 37°C. In these strains, nuclear accumulation of poly(A)$^+$ RNA and fragmentation of the nucleolus occurred rapidly following a shift to 37°C. Constitutive defects in nuclear pore complex distribution and nuclear structure were also seen in these strains. Although cells lacking Nup145p grew extremely slowly at 23°C and did not grow at 30°C, efficient growth at 23 or 30°C occurred as long as cells produced either the amino 58% or the carboxyl 53% of Nup145p. Strains carrying alleles of *NUP145* lacking up to 200 amino acids from the carboxy terminus were viable at 37°C but displayed nucleolar fragmentation and some nuclear accumulation of poly(A)$^+$ RNA following a shift to 37°C. Surprisingly, these strains grew efficiently at 37°C in spite of a reduction in the level of synthesis of rRNAs to approximately 25% of the wild-type level.

Macromolecules move between the nucleus and the cytoplasm through nuclear pore complexes (NPCs) (see references 9, 11, 13, 15, and 25 for recent reviews). NPCs are supramolecular structures that perforate the nuclear envelope, forming channels between the nucleus and the cytoplasm. Characterization of NPCs at the ultrastructural level has produced a model wherein two rings, one nuclear and one cytoplasmic, are joined by "spokes" that are arrayed to produce an eightfold symmetry around an axis perpendicular to the plane of the nuclear envelope (2, 23, 27). Filaments protruding from the cytoplasmic face of the pore and basket-like structures on the nuclear face have been observed in some preparations and have been implicated as potential docking sites for substrates that pass through the pore (17, 27, 35). Initial ultrastructural studies of *Saccharomyces cerevisiae* NPCs suggest many similarities between pores from yeast and metazoan cells (39). Yeast NPCs have a mass of approximately 66 mDa and may contain as many as 80 distinct polypeptide species (39).

Molecular characterization of individual nuclear pore proteins (nucleoporins, or NUPs) has been reported for more than 20 nucleoporins from *S. cerevisiae* and approximately 12 from vertebrate organisms (9, 40). Yeast nucleoporins and the genes encoding them have been isolated by a variety of strategies, including antibody screening of expression libraries, genetic synthetic lethal screens, and biochemical fractionation. We have identified several nucleoporins by screening a collection of yeast temperature-sensitive mutants for those with rapidly occurring defects in poly(A)$^+$ RNA export following a shift of cells to the nonpermissive temperature (3, 19, 22, 30). Interestingly, the genes for more than half of the identified yeast nucleoporins can be deleted individually without significantly affecting the growth of yeast cells at 23°C, though many of these strains do not grow or grow poorly at higher temperatures. This indicates that many yeast nucleoporins do not play essential roles under certain growth conditions. For the few known yeast nucleoporins that are essential, substantial portions of the nucleoporin can be deleted without abolishing growth at 23°C, but these partial deletions sometimes render the strain temperature sensitive (6, 32).

Among the yeast nucleoporins reported to be essential is Nup145p. *NUP145* was initially identified through a synthetic lethal screen using a mutant allele of the yeast nucleoporin gene *NSP1* (14) and, in a separate study, through its immunoreactivity with a monoclonal antibody which recognizes the GLFG family of vertebrate and yeast nucleoporins (47). A deletion-disruption of the N-terminal half (amino acids 1 to 550) of the *NUP145* protein led to abnormalities of nuclear

* Corresponding author. Mailing address: Department of Biochemistry, Dartmouth Medical School, 7200 Vail Building, Rm. 413, Hanover, NH 03755. Phone: (603) 650-1628. Fax: (603) 650-1128. E-mail: charles.cole@dartmouth.edu.
† Present address: Department of Genetics, University of Pennsylvania School of Medicine, Philadelphia, Pa.
‡ Present address: Department of Microbiology, Duke University, Durham, N.C.

pore distribution and nuclear envelope structure, but the mutant strain was still viable and grew well at temperatures between 17 and 37°C (47). In another study of *NUP145*, Fabre et al. replaced the portion of *NUP145* encoding amino acids 247 to 928 (of 1317) with the *HIS3* gene and found that the resulting strain was unable to grow at 30 or 37°C (14). This study also examined a domain of Nup145p containing a nucleoporin RNA-binding motif (NRM) centered around amino acids 490 to 500. This motif is similar to RNP-1 motifs, and like RNP-1 motifs was able to bind to RNA homopolymers (14). This result suggests that Nup145p might bind RNA in vivo and could play a direct role in RNA transport through the NPC. However, the Nup145p NRM and other similar motifs found in Nup100p and Nup116p were not essential, as judged by deletion analysis of these domains. Only when the NRM had been removed from Nup100p, Nup116p, and Nup145p was the strain unable to grow, and then only at elevated temperatures. When *NUP145* was placed under control of the inducible *GAL10* promoter, depletion of Nup145p by transfer of cells to glucose led to cessation of growth and resulted in gradual defects in export of poly(A)$^+$ RNA. Approximately 30% of the cells showed nuclear accumulation of poly(A)$^+$ RNA 3 h after repression of Nup145p synthesis, while 12 h was required for all cells to show nuclear accumulation of poly(A)$^+$ RNA. This depletion experiment further suggested a role for Nup145p in poly(A)$^+$ RNA trafficking, although such an experiment does not clearly identify a domain that may be responsible for the phenotype.

In this study, we attempted to define the essential domain of Nup145p and its role in RNA export by studying mutant alleles of *NUP145*. The current studies, taken together with previous findings that the first 550 amino acids of Nup145p are not required for growth of cells between 17 and 37°C (14, 47), indicate that there is no single domain of Nup145p required for growth at temperatures up to 30°C. Growth at 37°C and export of poly(A)$^+$ RNA required the presence of sequences within the carboxyl half of the protein. Constitutive clustering of NPCs was seen in most strains and morphological alterations to the nucleolus were seen in all strains carrying carboxyl truncations of Nup145p. Defects in nucleolar morphology did not necessarily correlate with defects in ribosome biogenesis, as judged by cell growth behavior and analysis of rRNA processing.

### MATERIALS AND METHODS

**Yeast strains, cell culture, mutant isolation, and genetic methods.** Yeast strains used in this study are listed in Table 1, and the plasmids used are listed in Table 2. Strains were cultured by standard methods (43), using rich (YPD) media or defined synthetic complete (SC) media lacking appropriate amino acids or nucleotides. Temperature-sensitive mutants were grown at 23°C (permissive temperature) or shifted to 37°C (restrictive temperature). Genetic procedures such as matings, sporulations, and plasmid transformations using electroporation were performed by standard techniques (21, 37).

Isolation of *RAT* mutants has been previously described (3). Briefly, temperature-sensitive yeast strains generated by exposure to UV light were shifted to a restrictive temperature for 2 h and examined by using indirect immunofluorescence to identify strains which accumulated poly(A)$^+$ RNA in their nuclei. Strains that exhibited accumulation of poly(A)$^+$ RNA within their nuclei were chosen for further study. Such mutants were then backcrossed against a wild-type strain at least three times. Only mutant strains which showed a cosegregation of temperature sensitivity and poly(A)$^+$ RNA trafficking defects in a 2:2 ratio were further analyzed.

**Cloning and mapping of *NUP145* and confirmation that the mutated gene is an allele of *NUP145*.** Strain AGY48 was transformed with a *URA3*-marked *S. cerevisiae* genomic library in YCp50, constructed by Rose et al. (36). Transformants were plated on SC medium lacking uracil at 37°C to select for transformants that had acquired a plasmid clone that could facilitate growth at the restrictive temperature. Plasmids were isolated from those transformants that grew at 37°C and examined. All complementing plasmids were related, based on restriction endonuclease digestion patterns. The plasmid clones were retested for

TABLE 1. Yeast strains used in this study

| Strain | Genotype | Source or reference |
|---|---|---|
| FY23 | *MAT***a** *trp1Δ63 leu2Δ1 ura3-52* | 51 |
| FY86 | *MAT*α *his3Δ200 leu2Δ1 ura3-52* | 51 |
| TDY102 | *MAT***a** *trp1Δ63 leu2Δ1 ura3-52 URA3* | This study |
| TDY105 | *MAT***a** *ura3-52 leu2Δ1 trp1Δ63 nup145-10* | This study |
| TDY120 | *MAT***a** *trp1Δ63 leu2Δ1 ura3-52 nup145-11* | This study |
| TDY121 | *MAT***a** *trp1Δ63 leu2Δ1 ura3-52 nup145-12* | This study |
| TDY122 | *MAT***a** *trp1Δ63 leu2Δ1 ura3-52 nup145-13* | This study |
| TDY123 | *MAT***a** *trp1Δ63 leu2Δ1 ura3-52 nup145-14* | This study |
| TDY124 | *MAT***a** *trp1Δ63 leu2Δ1 ura3-52 nup145-15* | This study |
| TDY131 | *MAT***a** *trp1Δ63 leu2Δ1 ura3-52 nup145-16* | This study |
| TDY132 | *MAT***a** *trp1Δ63 leu2Δ1 ura3-52 nup145-17* | This study |
| TDY133 | *MAT***a** *trp1Δ63 leu2Δ1 ura3-52 nup145-18* | This study |
| TDY134 | *MAT***a** *trp1Δ63 leu2Δ1 ura3-52 nup145-19* | This study |
| TDY150 | *MAT***a** *trp1Δ63 leu2Δ1 ura3-52 YCp50 URA3* | This study |
| TDY151 | *MAT***a** *trp1Δ63 leu2Δ1 ura3-52 nup145-10 YCp50 URA3* | This study |
| TDY154 | *MAT***a** *trp1Δ63 leu2Δ1 ura3-52 nup145-13 YCp50 URA3* | This study |
| TDY155 | *MAT***a** *trp1Δ63 leu2Δ1 ura3-52 nup145-14 YCp50 URA3* | This study |
| AGY10 | *MAT***a**/*MAT*α *his3Δ200/HIS3 leu2Δ1/leu2Δ1 ura3-52/ura3-52 TRP1/trp1Δ63 nup145-10/ NUP145* | This study |
| AGY48 | *MAT*α *his3Δ200 leu2Δ1 ura3-52 nup145-10* | This study |
| LGY101 | *MAT*α *his3Δ200 leu2Δ1 ura3-52 rat7-1* | 19 |
| OLY101 | *MAT*α *his3Δ200 leu2Δ1 ura3-52 rat3-1* | 30 |
| SWY29 | *MAT***a** *ade2-1 ura3-1 his3-11,15 trp1-1 leu2-3,112 can1-100 nup116-5::HIS3* | 48 |
| SWY77 | *MAT***a** *ade2-1 ura3-1 his3-11,15 trp1-1 leu2-3,112 can1-100 nup145-1::URA3* | 48 |
| ACY1 | *MAT*α/*MAT***a** *his3Δ200/his3Δ200 leu2Δ1/ leu2Δ1 ura3-52/ura3-52 trp1Δ63/TRP1* | Anita Corbett |
| CHY133 | *MAT*α *his3Δ200 leu2Δ1 ura3-52 NUP145:: HIS3* | This study |
| CHY136 | *MAT*α *his3Δ200 leu2Δ1 ura3-52 NUP145:: HIS3(LEU2 CEN NUP145-22$_{myc}$)* | This study |
| CHY137 | *MAT*α *his3Δ200 leu2Δ1 ura3-52 NUP145::HIS3(LEU2 CEN NUP145$_{myc}$)* | This study |

their ability to confer growth to AGY48 cells at 37°C and to correct the poly(A)$^+$ RNA trafficking defect associated with the parental mutation. Partial DNA sequence analysis indicated that the cloned gene was *NUP145*. To show that the cloned gene was complementing the mutation and not acting as a suppressor, a 7.0-kb *Sal*I fragment that contained the complementing activity was cloned into YIplac211 (16) and used to transform the wild type (FY23), with selection for Ura$^+$ prototrophs. The integrity of the recombination event and integration at the genomic *NUP145* locus were confirmed by Southern hybridization. This strain (TDY102) was mated with AGY48 and sporulated. Subsequent segregation analysis showed that uracil auxotrophy and temperature sensitivity cosegregated in 76 of 80 progeny analyzed, indicating that the cloned DNA was not acting as an extragenic suppressor and that AGY48 carried a temperature-sensitive allele of *NUP145*.

**Construction of a *NUP145* disruption.** A PCR-based gene deletion approach (5) was used to delete the *NUP145* gene. By PCR amplification, we generated a *HIS3* cassette that was flanked at its ends by 40 or 43 nucleotides identical to sequences just upstream and downstream of the *NUP145* open reading frame (ORF). The upstream oligonucleotide sequence was 5′ GCTTTTTAGAACCA CAAGCAAAGGAGAAGCAGTAGCCACCGGCCTCCTCTAGTACACTC 3′, and the downstream oligonucleotide sequence was 5′ CCTGGGCAAACTC ACCCCTCAAGTATGCCTTTTCTGGCTGCCCGCGCGCTCGTTCAGA A3′. For both oligonucleotides, the last 19 nucleotides are homologous to the *HIS3* selectable marker. We used 20 ng of the *HIS3*-containing plasmid pBM2815 (obtained from P. Silver, Dana-Farber Cancer Institute, Boston, Mass.) to generate the deletion construct in the PCR. The 50-μl reaction mixture consisted of 1× PCR buffer (10 mM Tris-HCl, 15 mM MgCl$_2$, 500 mM KCl; pH 8.3), 0.8 mM deoxynucleoside triphosphates (0.2 mM each dATP, dGTP, dCTP, and dTTP), 1 mM each upstream and downstream oligonucleotide, and 2 U of *Taq* DNA polymerase (Boehringer Mannheim Biochemicals). The reaction was subjected to a 30-cycle amplification consisting of 1.5 min at 94°C, 2.0 min at 50°C, and 2.0 min at 72°C. The PCR product was used to transform wild-type

TABLE 2. Plasmids used in this study

| Plasmid | Relevant characteristics | Source or reference |
|---|---|---|
| pTD1 | Library clone of *NUP145*; *URA3* Ap$^r$ Tc$^r$ | This study |
| pTD3 | 7.0-kb *Sal*I clone of *NUP145* into YCplac211 | This study |
| pTD6 | 5.5-kb *Sal*I-*Sph*I clone of *NUP145* into YCplac33 | This study |
| pTD10 | *nup145-10* allele cloned into YCplac111 | This study |
| pTD50 | Deletion of *NUP145* from *Bsp*EI to *Avr*II in YIplac211 | This study |
| pTD51 | Deletion of *NUP145* from *Eco*RV to *Avr*II in YIplac211 | This study |
| pTD52 | Deletion of *NUP145* from *Afl*II to *Avr*II in YIplac211 | This study |
| pTD53 | Deletion of *NUP145* from *Msc*I to *Avr*II in YIplac211 | This study |
| pTD54 | Deletion of *NUP145* from *Cla*I to *Avr*II in YIplac211 | This study |
| pTD70 | In-frame deletion of *NUP145* from *Afl*II to *Msc*I in YIplac211 | This study |
| pTD71 | In-frame deletion of *NUP145* from *Bsp*EI to *Afl*II in YIplac211 | This study |
| pTD73 | In-frame deletion of *NUP145* from *Eco*RV to *Msc*I in YIplac211 | This study |
| pTD74 | In-frame deletion of *NUP145* from *Msc*I to *Cla*I in YIplac211 | This study |
| pTD101 | In-frame insertion of a triple *myc* tag at codon 1292 of *NUP145* in YIplac211 | This study |
| pTD107 | In-frame deletion of codons 550–638 in *NUP145* in pTD101 | This study |
| pRAT10-7 | 5.5-kb *Sal*I-*Sph*I clone of *NUP145* into pUC18; Ap$^r$ | This study |
| pJJ248 | *TRP1* cassette plasmid | 28 |
| YIplac211 | Yeast integration vector; *URA3* Ap$^r$ | 16 |
| YCplac33 | Yeast *ARS-CEN* plasmid; *URA3* Ap$^r$ | 16 |
| YCplac111 | Yeast *ARS-CEN* plasmid; *LEU2* Ap$^r$ | 16 |

diploid strain ACY1, which is homozygous for *his3Δ200*. The flanking upstream and downstream sequences target the deletion construct to the *NUP145* locus such that the *NUP145* ORF is replaced with *HIS3* by homologous recombination. Recombinants were selected on SC-His plates, and recombination was verified by PCR. To determine whether *NUP145* was essential for vegetative growth at various temperatures, we sporulated the diploids, dissected tetrads, and scored four-spore tetrads for their ability to grow at 23, 30, and 37°C and for auxotrophic markers.

**Cloning of the *nup145-10* allele.** Gap repair (38) was used to clone the temperature-sensitive allele of *NUP145* from the parental mutant strain. Plasmid pTD6 was digested with various restriction enzymes, and the appropriate linear fragments were isolated from an agarose gel following electrophoresis and used to transform AGY48 for repair of the gap. Repaired gaps that failed to restore growth at a restrictive temperature to AGY48 delimited the mutation to a 1.6-kb span between the *Eco*NI and *Bsp*EI sites shown in Fig. 6A. Oligonucleotide primers were synthesized, and sequencing reactions were carried out on both strands with both wild-type and mutant alleles of *NUP145* used as templates. Sequencing reaction products were analyzed on an Applied Biosystems model 373A DNA sequencer.

**Construction of C-terminal mutants of *NUP145*.** C-terminal truncations were made by digesting pRAT10-7 (*NUP145* gene cloned into pUC18) with the following combinations of restriction endonucleases: *Bsp*EI/*Avr*II, *Eco*RV/*Avr*II, *Afl*II/*Avr*II, *Msc*I/*Avr*II, and *Cla*I/*Avr*II. In-frame deletions were constructed by digesting pRAT10-7 with *Bsp*EI/*Afl*II, *Eco*RV/*Msc*I, *Afl*II/*Msc*I, or *Msc*I/*Cla*I. In all cases, 3′ ends were filled in by using the Klenow fragment of DNA polymerase I and deoxyribonucleotides. Appropriate DNA fragments containing pUC18 and the appropriate portions of *NUP145* DNA were gel purified and recircularized by using T4 DNA ligase. Such manipulations produced 3′ truncations of *NUP145* resulting in the production of proteins truncated after amino acids 884 (*Bsp*EI/*Avr*II; *nup145-11*), 929 (*Eco*RV/*Avr*II; *nup145-12*), 979 (*Afl*II/*Avr*II; *nup145-13*), 1095 (*Msc*I/*Avr*II; *nup145-14*), and 1240 (*Cla*I/*Avr*II; *nup145-15*) and in-frame deletions of *NUP145* from codons 884 to 979 (*Bsp*EI/*Afl*II; *nup145-16*), 929 to 1095 (*Eco*RV/*Msc*I; *nup145-17*), 979 to 1095 (*Afl*II-*Msc*I; *nup145-18*), and 1095 to 1240 (*Msc*I/*Cla*I; *nup145-19*). The *Sal*I/*Sph*I fragments encoding the mutant forms of *NUP145* were separated from pUC18 sequences by agarose gel elec-

trophoresis and ligated with linearized YIplac211 DNA. For the in-frame deletions, the integrity of the reading frames was analyzed by DNA sequencing as described above. The above deletions were introduced into wild-type FY23 via "pop-in/pop-out" mutagenesis as described by Rothstein (38). Initial integrants and 5-fluoroorotic acid-resistant derivatives were analyzed via Southern hybridization to ensure integrity of the recombination events.

**In situ hybridization and immunofluorescence assays.** In situ hybridization assays for poly(A)$^+$ RNA localization and indirect immunofluorescence techniques for protein localization have been described previously (3, 8, 19, 30). Anti-Nop1p monoclonal antibody A66 (a gift from J. Aris, University of Florida, Gainesville) (4) was used at a 1:100 dilution; fluoresceinated horse anti-mouse immunoglobulin G (IgG) (Vector Laboratories, Inc., Burlingame, Calif.) was used as a secondary antibody at a 1:650 dilution. RL1 monoclonal antibody (a gift from L. Gerace, Scripps Research Institute, La Jolla, Calif.) (44) was used at a dilution of 1:400, and monoclonal antibody 2.3B against yeast fibrillarin (a gift from M. Snyder, Yale University, New Haven, Conn.) was used at a dilution of 1:10; for both of these, a fluorescein isothiocyanate (FITC)-conjugated goat anti-mouse IgM (Vector Laboratories, Inc.) was used at a dilution of 1:650. Antibody against Rat7p/Nup159p raised in guinea pigs (19) was used at a 1:2,000 dilution. FITC-conjugated goat anti-guinea pig IgG (Vector Laboratories, Inc.) was used at a 1:650 dilution.

**[³H]uridine incorporation and rRNA processing studies.** Yeast strains were analyzed for [³H]uridine incorporation by transforming them with a *URA3*-marked *ARS-CEN* plasmid and growing them in SC broth lacking uracil at 23°C until the cells reached an optical density at 600 nm of 0.3 to 0.5. Aliquots of each culture were maintained at 23°C or shifted to 37°C for 1 h before addition of label. A 160-μl volume of [³H]uridine (20.7 Ci/mmol; DuPont-NEN, Boston, Mass.) was added to 1.6 ml of culture, and the mixture was incubated at either 23 or 37°C for 10 min. Cells were then pelleted, the supernatant was removed, and the cell pellet was snap frozen in dry ice-ethanol before further processing. Total RNA was extracted from the cells, and the resulting RNA fractions were analyzed for trichloroacetic acid-precipitable counts according to a protocol from Sambrook et al. (41). rRNA processing was monitored by loading of approximately equal numbers of counts of RNA samples onto formaldehyde-agarose gels, separation of RNAs by electrophoresis, Northern transfer, and detection of RNA by using fluorography.

**Western blotting (immunoblotting).** Total cell extracts of yeast strains used were prepared as follows. Cultures were incubated in YPD medium at 23°C. Equivalent optical density units of each culture were then broken open by using a combination of glass bead disruption and boiling in a lysis-sample buffer consisting of 10% glycerol, 2% sodium dodecyl sulfate, 0.12 M Tris-Cl (pH 6.8), 8 M urea, and 0.7 M β-mercaptoethanol. Cells were boiled for 3 min in this buffer and then alternated between vortexing and boiling (15 s per treatment) five times. Insoluble material was pelleted, and the supernatants were collected for gel analysis. Samples separated on sodium dodecyl sulfate–5% polyacrylamide gels were transferred to polyvinylidene difluoride membranes (Bio-Rad Laboratories, Hercules, Calif.). The membranes were probed with anti-myc antibody 9E10 (as tissue culture supernatant) at a 1:10 dilution in phosphate-buffered saline containing 0.1% Tween 20, with 5% nonfat dry milk used as a blocking agent. Anti-mouse secondary antibody conjugated to horseradish peroxidase was used at a 1:3,000 dilution. Detection was performed with chemiluminescent reagents from Pierce Chemical Corp. (Rockford, Ill.).

**Electron microscopy.** Preparation of yeast cells for analysis by electron microscopy was performed by a modification of published procedures (7, 18, 30, 53). Cells were cultured at the permissive temperature in YPD broth to an optical density at 600 nm of 0.5. At this time, aliquots were shifted to 37°C for 1 h. Cells were harvested by filtration and were fixed for 2 h at room temperature in a 3% glutaraldehyde solution containing 0.1% tannic acid in 0.1 M sodium cacodylate, pH 6.8. The fixed cells were washed twice in 50 mM potassium phosphate buffer (pH 7.5) and then digested with 125 mg of Zymolyase 100T (Seikagaku America, Inc., Rockville, Md.) per ml in 50 mM potassium phosphate buffer (pH 7.5) for 40 min at 30°C. After two washes in 0.1 M sodium cacodylate (pH 6.8), the spheroplasted cells were treated with 2% OsO₄ in 0.1 M sodium cacodylate (pH 6.8) for 1 h on ice (some strains were embedded in 4% SeaPrep agarose prior to OsO₄ treatment). Samples were next washed three times in double-distilled water and treated for 1 h with 2% uranyl acetate in double-distilled water. The cells were dehydrated through graded ethanol and embedded in Spurr's medium (45). Thin sections were cut, stained with uranyl acetate and Reynold's lead citrate, and examined on a JEOL 100CX electron microscope at 60 or 80 kV accelerating voltage.

## RESULTS

**Nup145p is required for efficient mRNA export, yet no single domain is essential for growth.** During a screen for temperature-sensitive *S. cerevisiae* mutants which accumulated poly(A)$^+$ RNA in their nuclei at a restrictive temperature, we identified a mutant strain (AGY48) that was characterized by rapid nuclear accumulation of poly(A)$^+$ RNA in cells shifted to the nonpermissive temperature of 37°C. Figure 1 shows the
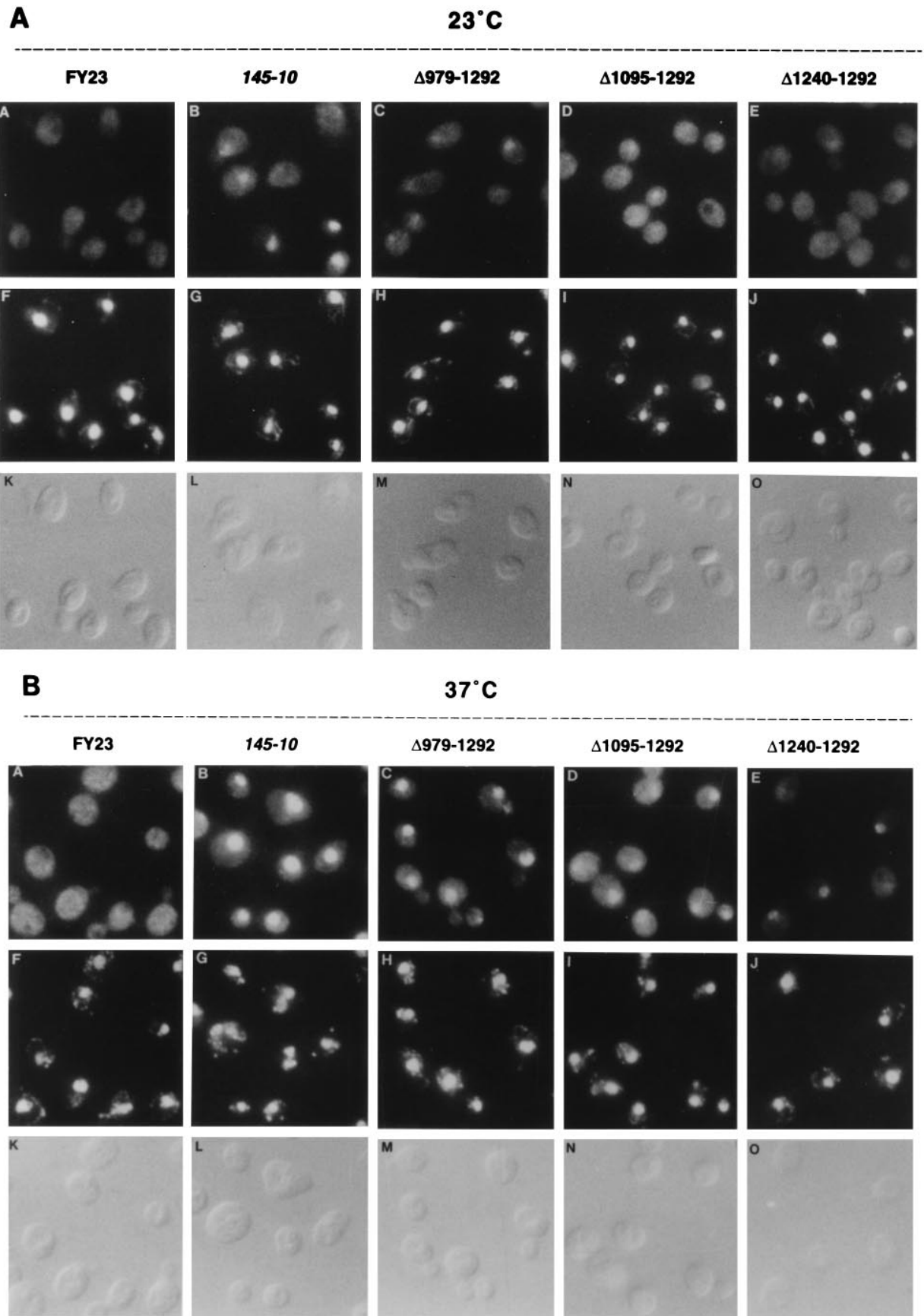
FIG. 1. Poly(A)$^+$ RNA distribution in wild-type cells and selected *NUP145* mutants. (A) Cells incubated and processed for poly(A)$^+$ RNA localization at 23°C. A to E, poly(A)$^+$ RNA localization; F to J, DAPI staining to mark the nuclear region of the same fields of cells as in panels A to E; K to O, Nomarski optics. (B) Cells processed for poly(A)$^+$ RNA localization after a 1-h shift to 37°C. A to E, poly(A)$^+$ RNA localization; F to J, DAPI staining of the same fields of cells shown in panels A to E; K to O, Nomarski optics. Exposure times and printing conditions were identical for all poly(A)$^+$ RNA localization panels.

909

results of an in situ hybridization assay comparing wild-type yeast cells with the mutant strain at both permissive and non-permissive temperatures. At the permissive growth temperature of 23°C, wild-type cells displayed relatively even fluorescence throughout the cell (Fig. 1A, panel A). A similar pattern was seen when wild-type cells were shifted to 37°C for 1 h (Fig. 1B, panel A). For the *nup145-10* mutant strain, significant nuclear accumulation of poly(A)$^+$ RNA was seen in approximately half the cells when they were cultured at 23°C (Fig. 1A, panel B); in different experiments, the percentage of mutant cells showing clear nuclear accumulation of poly(A)$^+$ RNA under permissive conditions varied, but nuclear staining was rarely as bright as following a shift of mutant cells to 37°C, and cytoplasmic staining was also always seen in mutant cells incubated at 23°C. After a shift to 37°C for 60 min (Fig. 1B, panel B), nearly 100% of the mutant cells displayed strong nuclear accumulation of poly(A)$^+$ RNA.

The mutation in AGY48 was recessive, as judged by analysis of growth of heterozygous diploids (AGY10) at 37°C and a lack of any mRNA trafficking defects at 37°C in the same cells (data not shown). A complementing wild-type allele of the mutated gene was obtained by transforming mutant cells with a yeast genomic library in the centromeric plasmid YCp50 (36). Partial sequencing of the complementing DNA showed that it encoded the yeast nucleoporin Nup145p. Nup145p contains an N-terminal domain consisting of 12 repeats identical or similar to the GLFG tetrapeptide repeat found in several other nucleoporins, a central region that includes a domain related to the RNP-1 class of RNA-binding proteins, and a C-terminal domain. The central domain of Nup145p, including the NRM, is similar to the central domains of Nup100p and Nup116p, though Nup100p and Nup116p are more closely related in this domain than either is to Nup145p. The long C-terminal domain of Nup145p is not shared with any yeast nucleoporins identified to date. To determine the nature of the mutation responsible for the phenotypic defects associated with the *nup145-10* allele, the genomic mutation was isolated by using gap repair (38). Sequence analysis located a nonsense mutation at codon 698 caused by a change of a TGG codon to TGA. The mutant allele in the *nup145-10* strain therefore encodes a Nup145p truncated at amino acid 698. This mutant protein lacks the C-terminal 47% of Nup145p.

Earlier studies with *NUP145* had reported that it was essential because a strain containing the *HIS3* gene in place of residues 247 to 928 was unable to grow at 30 or 37°C (14), yet 40% of the N terminus could be replaced with protein A (14) or disrupted with a *LEU2* gene (47) without significantly affecting growth of cells at temperatures between 17 and 37°C. The nature of the mutant Nup145p encoded by the *LEU2*-disrupted allele is unknown because the allele contains the *LEU2* gene between the *NUP145* promoter and the C-terminal 60% of the gene. It is also uncertain whether the allele containing *HIS3* in place of residues 247 to 928 produces any functional fragments of Nup145p. Therefore, we generated a disruption allele containing the *HIS3* gene in place of the entire Nup145p ORF and compared the growth of this strain (CHY133) with that of the wild type (FY86) and the strain carrying the *nup145-10* allele at 23, 30, and 37°C (Fig. 2A). Strain CHY133 (Δ*nup145*) grew very slowly at 23°C and could not grow at 30 or 37°C. This confirms that *NUP145* is essential for normal growth of yeast cells at all temperatures tested. Cells carrying the *nup145-10* allele grew with doubling times of 4 to 5 h at 23°C and 6 to 7 h at 30°C, compared to the 2- to 2.5-h doubling time for the wild-type strain at 23 and 30°C. These cells underwent rapid cessation of division following a shift to 37°C. Cells which had been shifted to 37°C for various periods were plated on YPD medium and incubated at 23°C to determine how incubation at the nonpermissive temperature
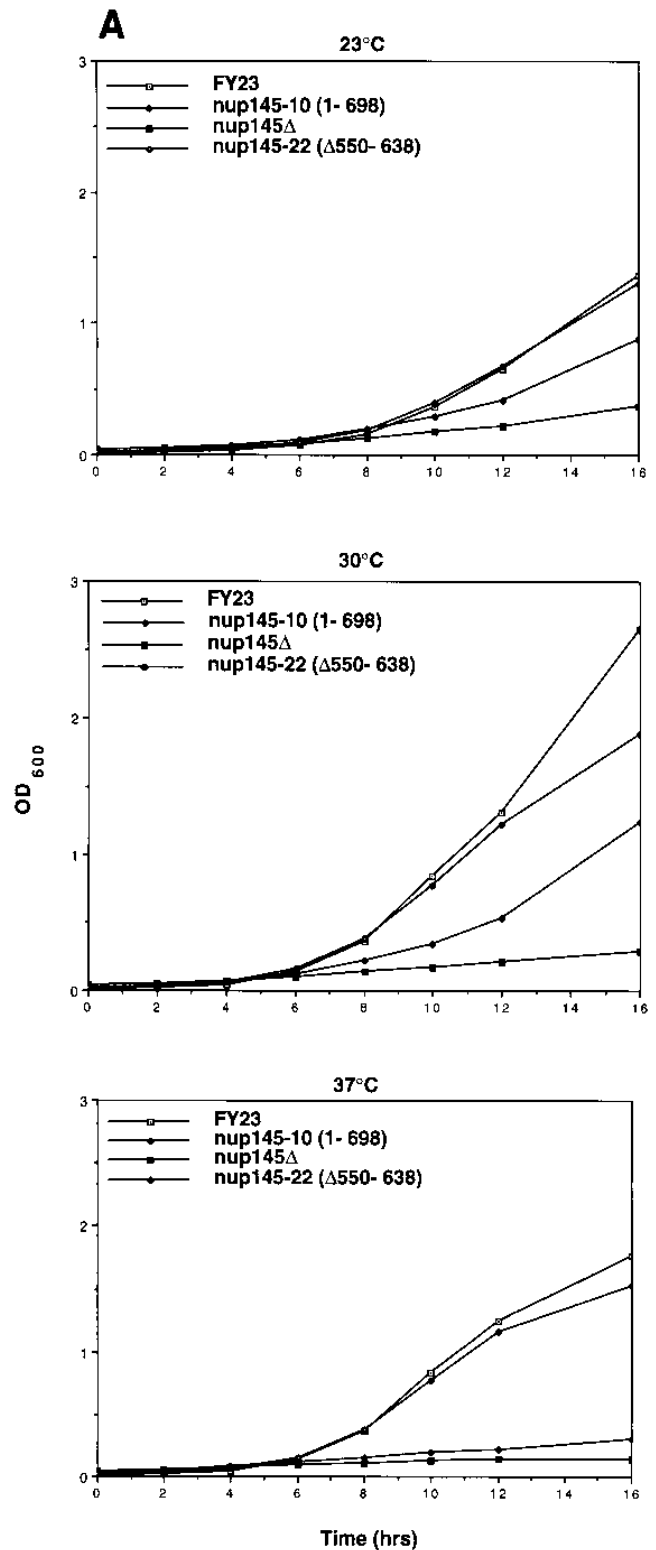


FIG. 2. Growth characteristics of *NUP145* mutant cells. (A) Growth curves of wild-type (FY23), *nup145-10* (AGY48; 1-698), and *nup145-22* (CHY136; Δ550-638) strains and cells carrying a complete disruption of the Nup145p ORF (CHY133). Cultures were grown at 23°C to mid-log phase in YPD medium and then split and allowed to resume growth at 23°C for 2 h. Half the cultures were then shifted to 30 or 37°C. Aliquots were removed at the indicated times, and the optical density at 600 nm (OD$_{600}$) was determined. (B) Growth properties of wild-type (FY23), *nup145-10* (AGY48; 1-698), *nup145-22* (CHY136; Δ550-638), *nup145-14* (TDY123; Δ1095-1292), and *nup145*Δ (CHY133) cells on YPD plates at the indicated temperatures. The *nup145*Δ (CHY133) cells form colonies on YPD plates at 23°C but cannot do so at 30 or 37°C. The plates were photographed after 2 days of growth.
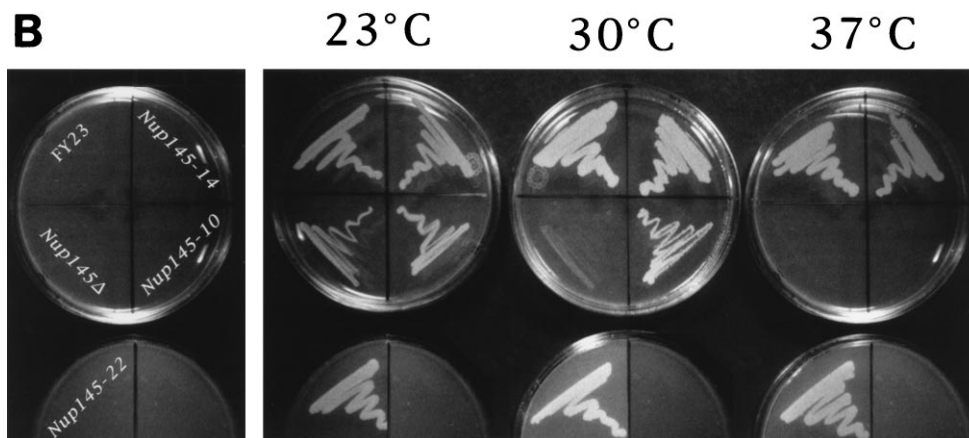
FIG. 2—*Continued.*

affected cell viability. *nup145-10* cells shifted to 37°C suffered an irreversible terminal defect; only 50% of cells incubated for 4 h at 37°C remained viable. After incubation at 37°C for an additional 20 h, fewer than 10% of the cells remained viable. In contrast, wild-type cells continued to double during incubation at 37°C.

These and earlier findings (14, 47) indicate that neither the first 550 nor the last 620 amino acids of Nup145p were required for growth at 23 or 30°C. To determine whether the remaining, central portion of Nup145p was essential, we constructed mutants with in-frame deletions of amino acids 550 to 638 and 550 to 698 (Δ550-638 and Δ550-698, respectively) and introduced plasmids encoding these mutant proteins into cells carrying a complete disruption of *NUP145*. The Δ550-638 allele permitted growth of the null strain at 23, 30, and 37°C at rates that were slightly lower than those of the wild type (Fig. 2A). The Δ550-698 strain behaved identically (data not shown). Figure 2B compares growth on plates of wild-type yeast (FY23) and strains carrying the complete disruption of *NUP145* (Δ*nup145*), the original temperature-sensitive allele (Δ698-1317; *nup145-10*), and the Δ550-638 allele (*nup145-22*). While *NUP145* is essential for normal growth at all temperatures tested, we conclude that there is no single region of Nup145p required for efficient growth at 23 or 30°C. Sequences within the carboxyl half of the molecule were required for growth at 37°C.

We next determined the localization of poly(A)$^+$ RNA in cells carrying either a complete disruption of *NUP145* or carrying the *nup145-22* (Δ550-638) allele. In the Δ*nup145* strain, nuclear accumulation of poly(A)$^+$ RNA was readily detected in many cells from the culture incubated at 23°C, but a cytoplasmic signal was also clearly evident. Following a shift to 37°C for 1 h, the nuclear signal was brighter in most cells. Those cells which did not show a nuclear signal also did not stain with DAPI (4′,6-diamidino-2-phenylindole) (Fig. 3), suggesting that the slow growth of this strain reflects a slight excess of cell division over cell death. The localization of poly(A)$^+$ RNA in cells carrying the *nup145-22* allele was the same as that in wild-type cells both at 23°C and after a shift to 37°C for 1 h.

**Nuclear ultrastructure abnormalities associated with the *nup145-10* allele.** Analysis of several yeast nucleoporin deletion mutants has revealed that mutant strains often have abnormalities of nuclear pore distribution, morphology, and/or nuclear envelope structure (12, 19, 30, 48). Aggregation of NPCs was seen in cells lacking ~500 N-terminal residues of Nup145p, based on studies by both immunofluorescence and electron

microscopy (47). In such cells, NPCs were observed to be packed into clusters, sometimes causing distention of the surrounding nuclear envelope. We analyzed cells carrying the *nup145-10* allele by indirect immunofluorescence at both permissive and nonpermissive temperatures, using the RL1 monoclonal antibody, which reacts with nucleoporins from both vertebrate and yeast cells (8, 44). In contrast to the punctate pattern of staining typical of NPCs seen in wild-type cells at either 23°C (Fig. 4A, panel A) or 37°C (data not shown), cells carrying the *nup145-10* allele displayed clearly discernible concentrations of fluorescent signal at a limited portion of nuclear rim (Fig. 4A, panel C), which indicates an abnormal distribution of NPCs. In wild-type cells, little fluorescent signal was seen in the cytoplasm, while cytoplasmic staining was considerably more pronounced in mutant cells.

To further examine this phenotype, *nup145-10* cells were processed for thin-section electron microscopy. Cells were incubated at the permissive temperature or shifted to 37°C for 1 h, a time at which mRNA trafficking defects were detected in all mutant cells. Under both incubation conditions, NPCs were observed to cluster towards one pole of the nucleus, as suggested from the immunofluorescence studies (Fig. 4B, panels B and C). These NPCs appeared to be essentially intact at the level of resolution afforded by these micrographs. Thus, complete pores were clustered as opposed to particular NPC antigens being mislocalized. The NPCs in *nup145-10* cells appeared to remain largely within the plane of the nuclear envelope. Distentions of the nuclear envelope formed by NPCs stacking on top of each other, as has been observed for an N-terminal deletion of *NUP145* (47), were not observed with the *nup145-10* allele. Occasional defects in overall nuclear morphology were observed. Some appeared to be due to invaginations of the nucleus (data not shown). Other defects appeared as protrusions of the nucleus extending from the main body of the nucleus (Fig. 4B, panel D). These deformities were seen at both incubation temperatures, indicating that they are constitutive. Similar abnormalities of nuclear structure have been seen for the *nup1-106* allele (6) and the *rat9-1/nup85-1* allele (18).

Use of an antifibrillarin antibody, which stains the yeast nucleolus, often in a crescent-shaped pattern (Fig. 5), showed that in the *nup145-10* mutant, the nucleolar staining pattern fragmented when mutant cells were shifted to 37°C for 60 min (Fig. 5E). The kinetics of this fragmentation were similar to the kinetics of enhanced poly(A)$^+$ RNA accumulation. While a moderate fraction of *nup145-10* cells accumulated poly(A)$^+$
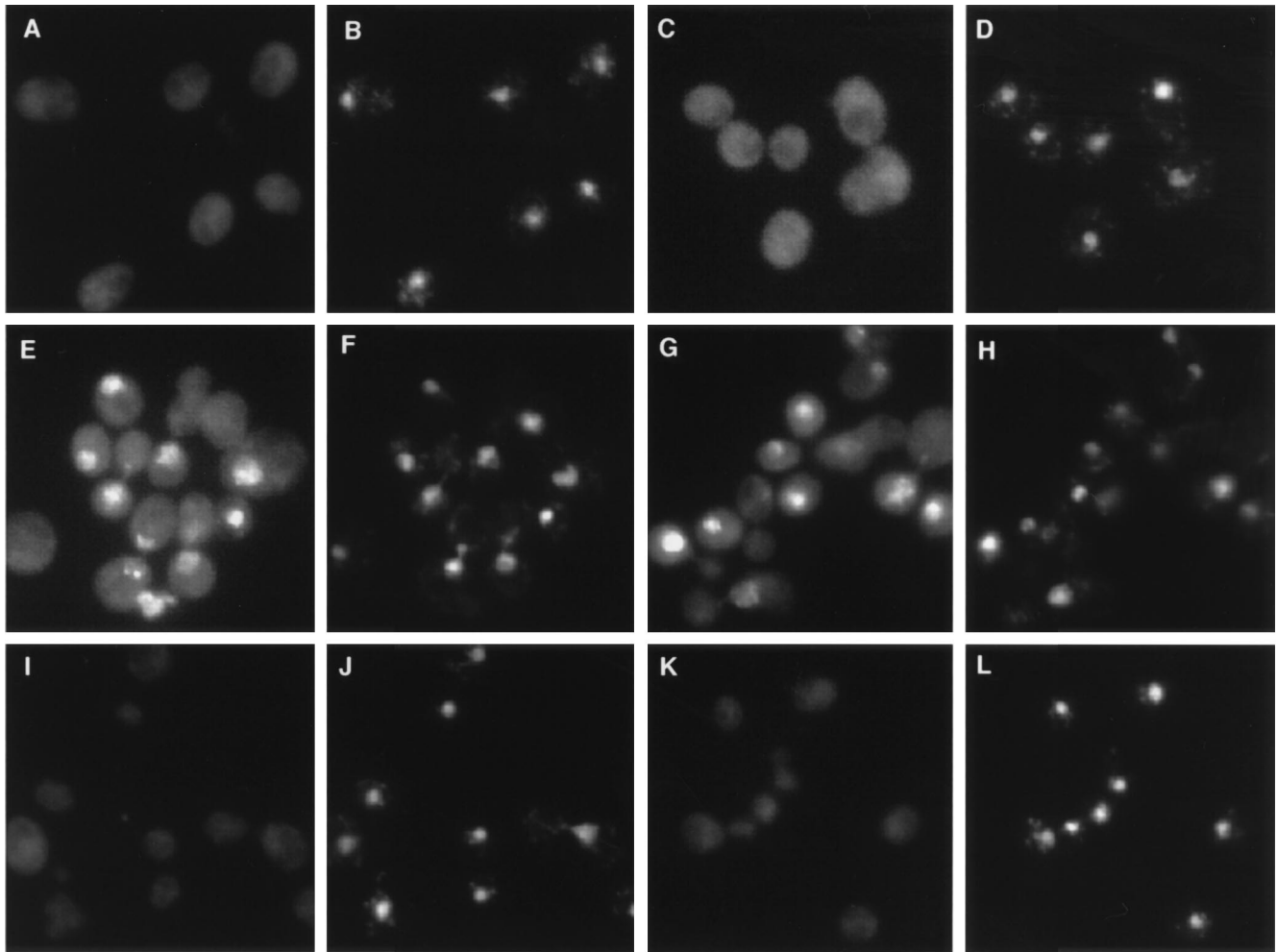
FIG. 3. In situ hybridization to examine the subcellular distribution of poly(A)$^+$ RNA in cells carrying a null allele of *NUP145* or a small internal deletion mutation. Wild-type (FY23) (A to D), *nup145Δ* (E to H), and *nup145-22* (Δ550-638) (I to L) cells were grown to mid-log phase at 23°C before fixation with formaldehyde. Panels A, C, E, G, I, and K show fluorescence signal representing the distribution of poly(A)$^+$ RNA. Panels B, D, F, H, J, and L show the same fields of cells counterstained with DAPI. Cells were either grown at 23°C (A, B, E, F, I, and J) or shifted to 37°C for 1 h (C, D, G, H, K, and L).

RNA in their nuclei during growth at 23°C, fragmentation of the nucleolus was not detected in cells grown at this temperature (Fig. 5C). The nucleolar fragmentation phenotype was observed by electron microscopy as well (Fig. 5I) where multiple fragments of the nucleolus can be seen. Even though nucleoli were disrupted, the ultrastructure of the nucleolar fragments in these cells is quite similar to that of wild-type nucleoli (compare Fig. 4B, panel B, with Fig. 5I). Interestingly, the nucleolus in some (Fig. 5I) but not all mutant cells appeared detached from the nuclear envelope, while in wild-type cells, the nucleolus was normally closely apposed to the nuclear envelope (data not shown).

**Analysis of C-terminal truncations of Nup145p.** A C-terminal truncation removing 47% of Nup145p produced the pleiotropic defects described above. To understand further the role of the carboxyl half of Nup145p and to assess whether any specific domains within the C terminus of Nup145p were responsible for any particular phenotype, a series of C-terminal truncations and in-frame deletions of the 3′ half of the *NUP145* gene was constructed. All alleles were integrated into the yeast genome in place of the wild-type *NUP145* gene by using pop-in/pop-out marker exchange (38) except for

*nup145-22* and *nup145-23*, which were examined on *CEN* plasmids in the strain carrying a complete disruption of *NUP145*. Figure 6A shows a map of the deletion alleles constructed for this study, while Fig. 6B compares the growth of some of these strains with that of the wild type (FY23) at 37°C. Strains whose Nup145 proteins were truncated at position 884, 929, or 979 grew as well as the *nup145-10* strain at 23 and 30°C and, like the *nup145-10* strain, were unable to grow at 37°C. In-frame deletions where any codons upstream of codon 979 were removed were also temperature sensitive and had defects similar to the aforementioned C-terminal truncations (data not shown), indicating that some portion of the protein between amino acids 698 and 979 is essential for function of Nup145p at 37°C. Strains containing either of two C-terminal deletions of Nup145p, one that extended from codons 1095 to 1292 (*nup145-14*) and one that spanned codons 1240 to 1292 (*nup145-15*), retained the ability to grow at 37°C (Fig. 6B).

These alleles of *NUP145* were examined for poly(A)$^+$ RNA trafficking defects as well as nucleolar structure and NPC distribution. Strains carrying temperature-sensitive alleles all displayed strong poly(A)$^+$ RNA trafficking defects, nucleolar fragmentation, and abnormal distribution of NPCs, pheno-
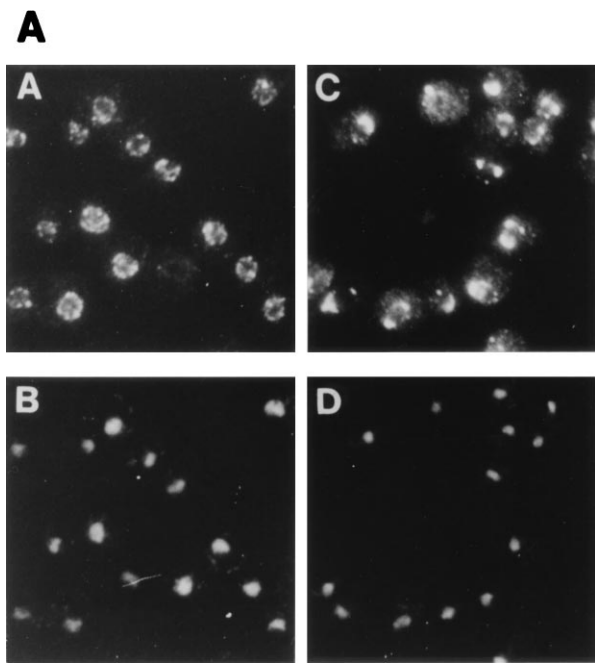
**A**



FIG. 4. NPCs are abnormally distributed in *nup145-10* cells (AGY48). (A) Wild-type (FY23) and *nup145-10* (1-698) cells were grown to mid-log phase at 23°C before fixation with formaldehyde. NPCs were localized by indirect immunofluorescence using the RL1 monoclonal antibody. Panels A and C show fluorescent signal from cells probed with FITC-conjugated anti-mouse IgM antibody. Panels B and D show the same fields of cells counterstained with DAPI. Panels A and B, wild type, 23°C; panels C and D, *nup145-10*, 23°C. (B) Thin-section electron micrographs of wild-type (A) and *nup145-10* (B to D) cells. Cells were grown either at 23°C (A, B, and D) or shifted to 37°C for 1 h (C) before fixation and preparation for electron microscopy. Individual NPCs (A) or clusters of NPCs (B and C) are indicated (arrowheads). C, cytoplasm; n, nucleus; no, nucleolus. Scale bars, 0.5 μm.

**B**
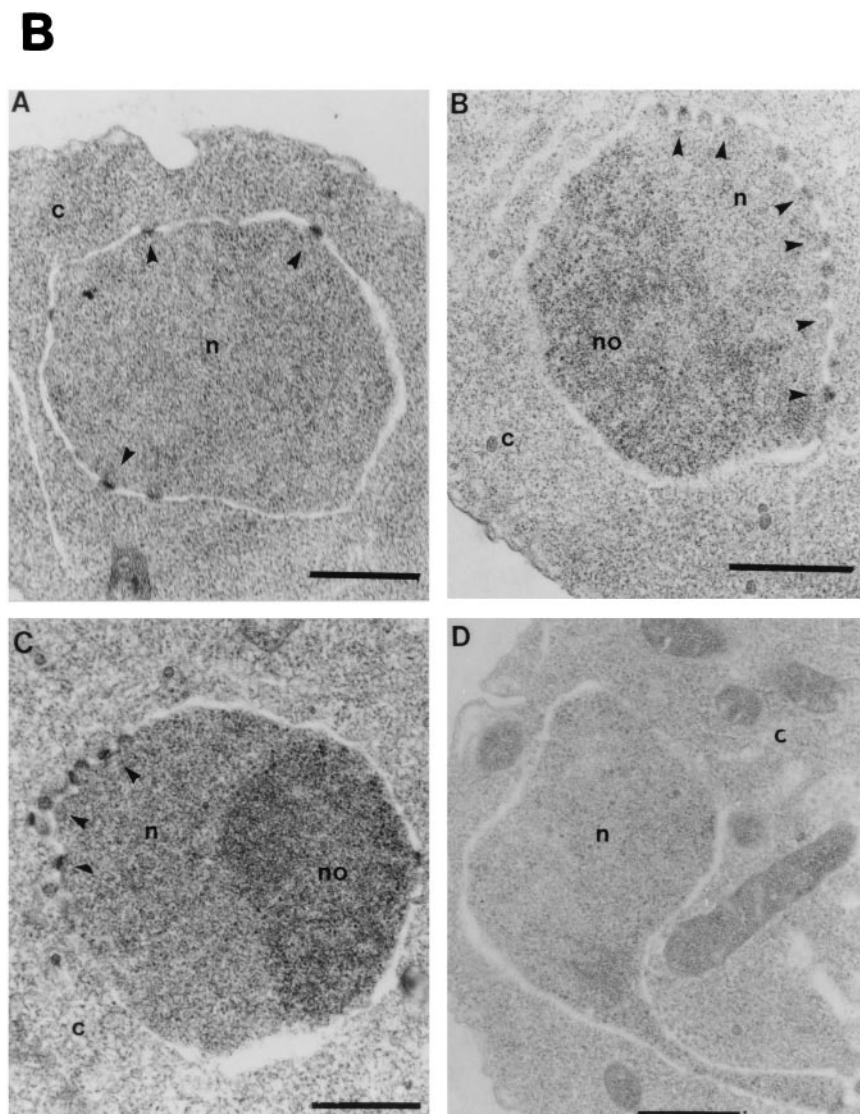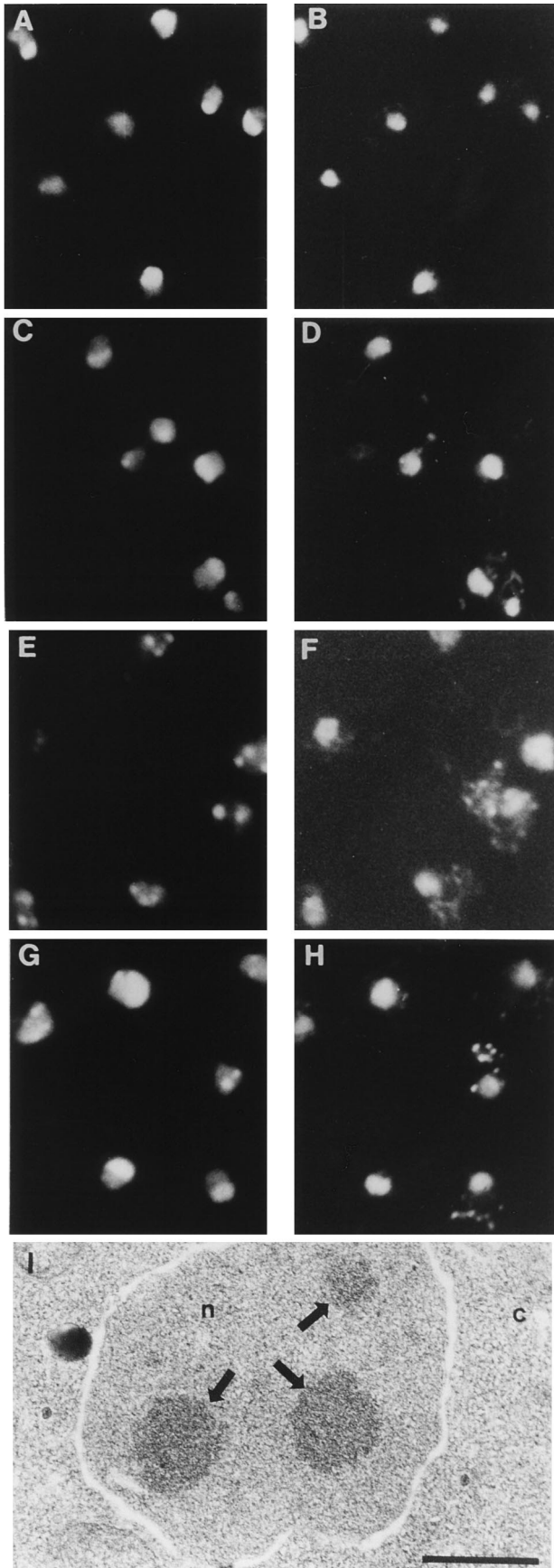
types that very closely resembled those caused by the *nup145-10* mutation. Strains harboring either the *nup145-14* (Δ1095-1292) or the *nup145-15* (Δ1240-1292) non-temperature-sensitive allele showed modest but clear accumulation of poly(A)$^+$ RNA in their nuclei following a 1-h shift to 37°C (Fig. 1B, panels D and E). This nuclear signal was weaker than the nuclear signal observed with strains harboring temperature-sensitive alleles of *NUP145* (Fig. 1B, panels B and C) and was present in about 60 to 80% of the cells. Neither the levels of nuclear accumulation of poly(A)$^+$ RNA in strains with the non-temperature-sensitive alleles nor the percentage of cells showing the phenotype increased noticeably upon longer incubation at 37°C (data not shown).

Immunofluorescence assays were performed to analyze NPC distribution in some of these strains. NPC distribution appeared wild type in cells carrying the *nup145-22* allele (Δ550-638) (Fig. 7A, compare panels G and A) but was highly abnormal in cells carrying a complete disruption of *NUP145* (Fig. 7A, panel E). No defects in NPC distribution were seen in cells carrying the non-temperature-sensitive allele *nup145-14* (Δ1095-1292) or *nup145-15* (Δ1240-1292) (data not shown). We also examined NPC distribution and cellular ultrastructure in some of these strains by electron microscopy (Fig. 7B). Cells carrying the *nup145-22* deletion (Δ550-638) (Fig. 7B, panel B) were indistinguishable from the wild type (Fig. 7B, panel A). Cells carrying a complete disruption of *NUP145* displayed clustered NPCs (Fig. 7B, panels C and D). In addition, we consistently observed a high degree of vacuolation in cells carrying a disruption of *NUP145* (data not shown).

Full-length Nup145p cannot be detected in wild-type cells (14, 47). Antibodies that recognize the GLFG repeat-containing family of nucleoporins identify a 65-kDa protein on Western blots which represents the amino-terminal portion of Nup145p (14, 47). A second polypeptide of 80 kDa derived from the carboxyl region of Nup145p represents the other half of the molecule (14, 47). It is not known whether these two fragments of Nup145p are generated by proteolytic processing during NPC biogenesis or represent cleavage during the preparation of protein extracts. Larger forms have been detected in extracts or in bacteria expressing Nup145p only when the amino-terminal 247 or 550 amino acids were replaced with protein A (14). We therefore performed Western blot analysis with Nup145p and the internal deletion mutant protein encoded by the *nup145-22* allele (Δ550-638). Both carried a myc epitope tag at their carboxyl termini. In wild-type cells, a fragment of Nup145p which migrated slightly more slowly than the 66-kDa marker was observed (Fig. 8). This represents the 80-kDa C-terminal half of Nup145p. In contrast, a protein with a mobility of approximately 130 kDa was seen in *nup145-22* cells, representing full-length mutant Nup145p. This indicates that deletion of amino acids 550 to 638 blocked the cleavage or

FIG. 5. The nucleolus becomes disorganized in *nup145-10* (AGY48) cells upon a shift to the nonpermissive temperature. Wild-type (FY23) and *nup145-10* (AGY48; 1-698) cells were grown to mid-log phase at the permissive temperature of 23°C and then subjected to various temperature conditions before fixation with formaldehyde. Nucleoli were visualized by indirect immunofluorescence using an anti-Nop1 monoclonal antibody. Panels A, C, E, and G show fluorescent signal from cells probed with FITC-conjugated anti-mouse IgG antibody after hybridization. Panels B, D, F, and H show the same fields of cells counterstained with DAPI. (A and B) Wild type, 23°C; (C and D) *nup145-10*, 23°C; (E and F) *nup145-10*, 30 min at 37°C; (G and H) *nup145-10*, 60 min at 37°C followed by 4 h at 23°C. Panel I is a thin-section electron micrograph of a *nup145-10* cell examined on a JEOL100CX electron microscope. These cells were shifted to 37°C for 60 min. The nucleolar fragments (see Materials and Methods) are indicated (arrows). n, nucleus; c, cytoplasm. Scale bar, 0.5 μm.
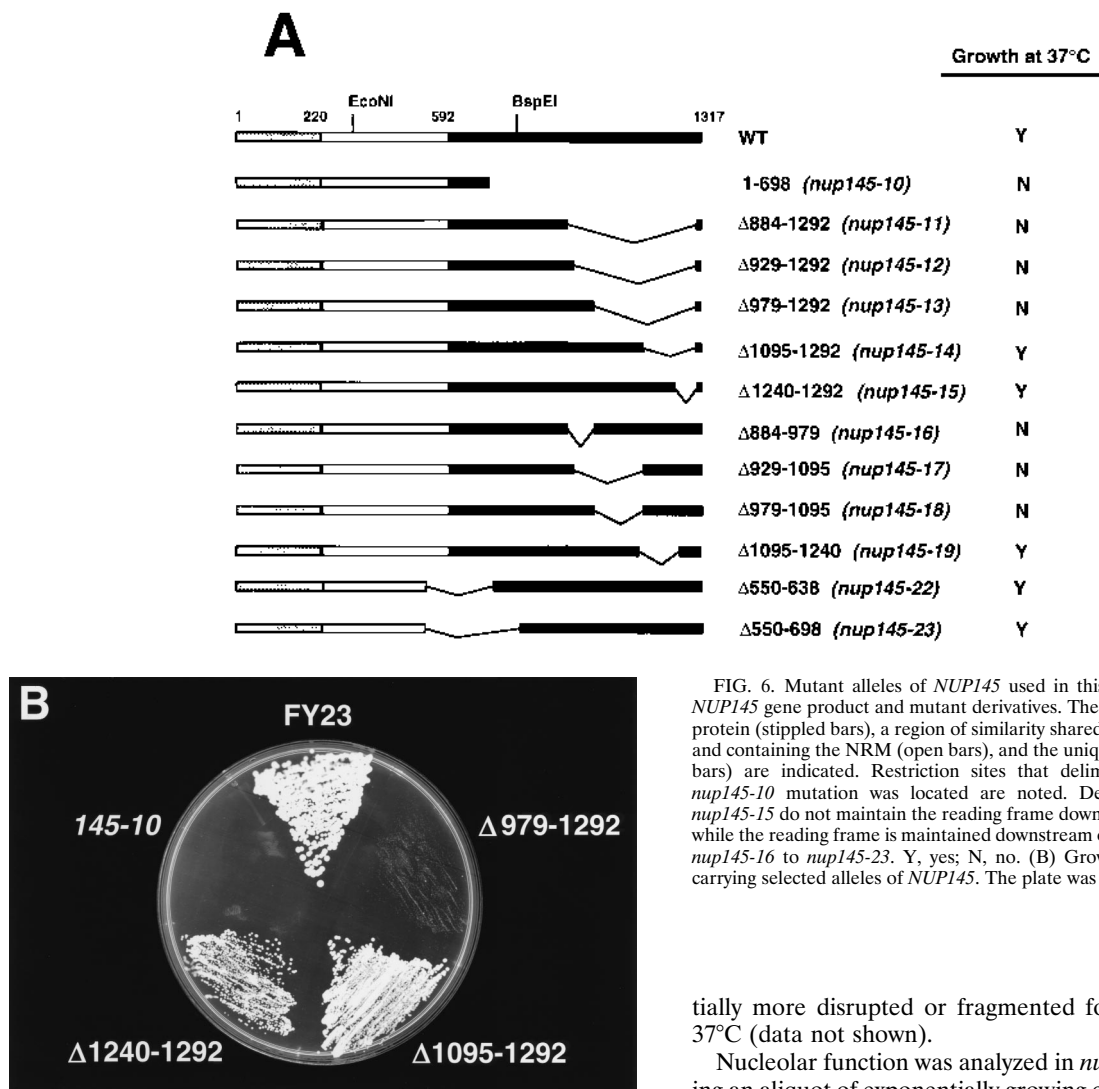
FIG. 6. Mutant alleles of *NUP145* used in this study. (A) Diagram of the *NUP145* gene product and mutant derivatives. The GLFG repeat domain of the protein (stippled bars), a region of similarity shared with Nup100p and Nup116p and containing the NRM (open bars), and the unique domain of Nup145p (solid bars) are indicated. Restriction sites that delimited the region where the *nup145-10* mutation was located are noted. Deletion alleles *nup145-11* to *nup145-15* do not maintain the reading frame downstream of the deleted region, while the reading frame is maintained downstream of deleted regions with alleles *nup145-16* to *nup145-23*. Y, yes; N, no. (B) Growth characteristics of strains carrying selected alleles of *NUP145*. The plate was incubated at 37°C for 2 days.

proteolysis of Nup145p, yet this protein was still efficiently incorporated into NPCs, as judged by indirect immunofluorescence (Fig. 7A, panel G), and must have functioned well, since cells carrying this allele grew nearly as well as wild-type cells at temperatures between 23 and 37°C.

**Nucleolar fragmentation, [³H]uridine incorporation, and rRNA processing in *NUP145* mutants.** The nucleolus is the domain within the nucleus where rRNA is transcribed, processed, and assembled into ribosomal subunits (reviewed in reference 52). If the nucleolar fragmentation phenotype observed in mutants shifted to 37°C were correlated with defects in ribosome biogenesis, this would likely be incompatible with growth, yet alterations to nucleolar morphology were also seen after a shift to 37°C of *nup145-14* and *nup145-15* cells (data not shown), which continued to grow well following the temperature shift (Fig. 2 and 6B). No alterations to nucleolar morphology were seen in cells carrying the *nup145-22* allele (Δ550-638), consistent with its wild-type growth properties at 23 and 37°C. In contrast, cells carrying a complete disruption of *NUP145* had some alterations in nucleolar morphology even when incubated continuously at 23°C, and nucleoli became substan-

tially more disrupted or fragmented following a 1-h shift to 37°C (data not shown).

Nucleolar function was analyzed in *nup145* mutants by shifting an aliquot of exponentially growing cells to 37°C for 1 h and pulse-labeling with [³H]uridine. We monitored the incorporation of label into trichloroacetic acid-insoluble material and examined rRNA synthesis and processing by electrophoretic analysis of labeled RNA. Following a shift to 37°C, [³H]uridine incorporation in *nup145-10* cells was reduced within 1 h to 5% of the level seen in the same cells at 23°C. Incorporation of [³H]uridine into RNA was reduced to approximately 18% of the wild-type level in cells harboring the temperature-sensitive Δ979-1292 allele of *NUP145*. Surprisingly, [³H]uridine incorporation was reduced to almost the same extent (to ~25% of wild-type levels) in cells carrying the non-temperature-sensitive Δ1095-1292 allele.

Labeled total cellular RNA was fractionated on formaldehyde-agarose gels, blotted onto nylon, and examined by fluorography. Processing of rRNA precursors to the 25S product appeared very similar in wild-type and mutant cells incubated at 23°C (Fig. 9, lanes 1, 3, and 5) or shifted to 37°C (lanes 2, 4, and 6). Processing of 20S to 18S rRNA is believed to occur in the cytoplasm in yeast (46) and appeared to be slightly impaired at 37°C in a strain with the temperature-sensitive Δ979-1292 allele (lane 4), while the ratio of 20 to 18S rRNA in a strain with the non-temperature-sensitive Δ1095-1292 allele (lane 6) appeared identical to that of a wild-type strain (lane 2). We conclude that the alterations observed in nucleolar
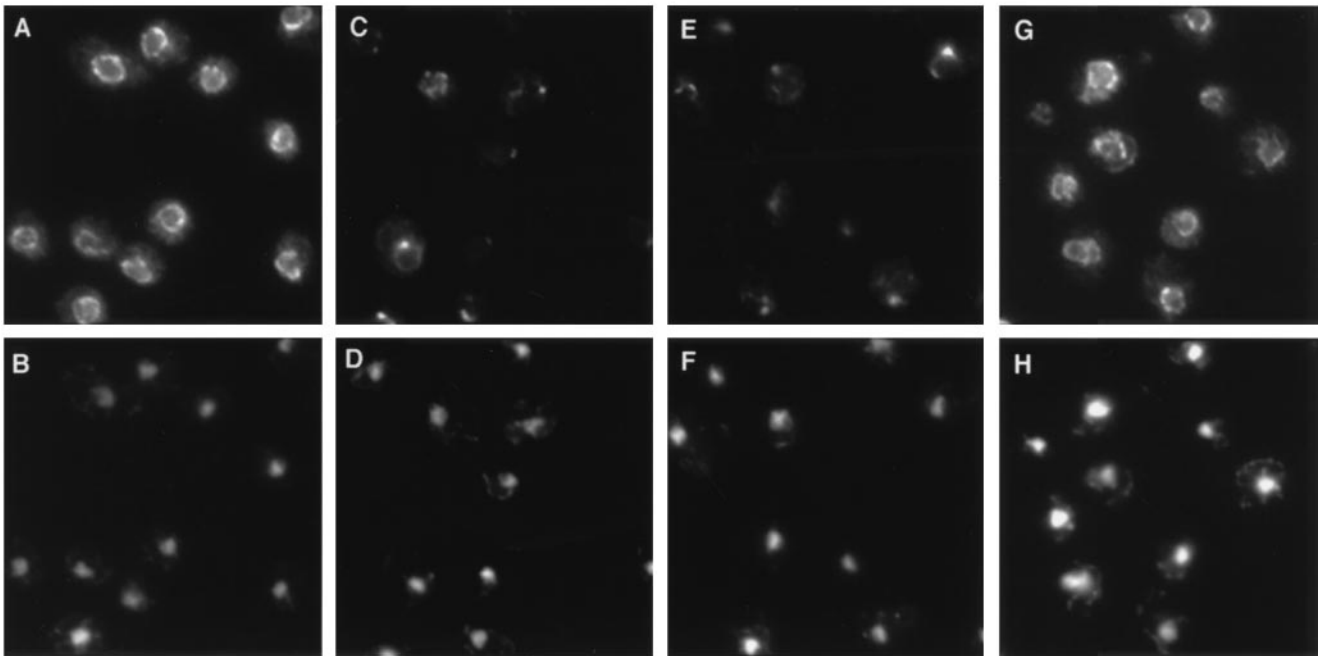
FIG. 7. (A) NPCs are clustered in cells with the *nup145-10* (TDY105) and the *nup145Δ* (CHY133) mutations. Indirect immunofluorescence was performed on wild-type (FY23) (A and B), *nup145-10* (TDY105) (C and D), *nup145Δ* (CHY133) (E and F), and *nup145-22* (CHY136; Δ550-638) (G and H) cells grown continuously at 23°C, using antiserum raised against a glutathione *S*-transferase-Rat7p/Nup159p fusion protein (A, C, E and G). Cells were counterstained with DAPI to visualize nuclei (B, D, F and H). (B) Electron microscopy of *NUP145* mutant cells examined on a JEOL 100CX. Cells were grown at room temperature and processed for electron microscopy. Wild-type (A) and *nup145-22* (B) cells show wild-type distribution of NPC. Cells with a disruption of *NUP145* (C and D) show clustered NPCs. Individual NPCs or clusters of pores are indicated (arrows). Scale bar, 0.5 μm.

morphology do not necessarily correlate with complete loss of rRNA synthesis and its normal processing.

## DISCUSSION

The goal of our studies is to identify yeast genes whose products participate directly in nucleocytoplasmic trafficking of mRNA or play important roles in modulating mRNA export. NPCs transport both proteins and RNA or RNP, and it seems likely that certain components of the NPC play a direct role in the translocation of RNA or RNP substrates through the pore. Our screen for mutants defective in this process identified the *nup145-10* allele of the nucleoporin *NUP145*, which results in a C-terminal truncation of the protein. Although previous studies have described *NUP145* (14, 47), neither of those studies examined the role of the C-terminal region of the protein.

Here, we report the characterization of novel mutant alleles of *NUP145*. A mutation of *NUP145* that produced rapid and strong temperature-dependent nuclear accumulation of poly(A)$^+$ RNA resulted from a nonsense mutation at codon 698 that truncated Nup145p to 53% of its wild-type size. All cells with C-terminal truncations of Nup145p examined showed nuclear accumulation of poly(A)$^+$ RNA at 37°C, although the strength of the nuclear signal was dependent upon the extent of truncation (Fig. 1). Most of the C-terminal truncations produced NPC clustering, and all showed nucleolar fragmentation when cells were shifted to 37°C. Mutations that deleted more central regions of the protein (amino acids 550 to 698) did not exhibit any of the phenotypes associated with the C-terminal mutations but did appear to block a proteolytic processing event that may occur in vivo.

**Does Nup145p function as one or two proteins?** Studies by Wente and Blobel (47) and Fabre et al. (14), as well as data presented here, suggest that Nup145p may be cleaved in vivo to form polypeptides of ~65 and ~80 kDa. Our studies show that this putative cleavage is not essential for the function of Nup145p, since cells carrying a deletion within the central part of *NUP145* that blocks proteolysis showed normal growth at all temperatures tested and had no obvious poly(A)$^+$ RNA trafficking defects (Fig. 3). A similar conclusion was also reached by Fabre et al. (14).

If Nup145p is proteolytically processed in vivo, then Nup145p would actually represent two nucleoporins that have a novel proteolytic pathway of biosynthesis. Loss of the N-terminal p65 portion appears to resemble the phenotypes caused by deletion of *NUP100* or *NUP2*, in that none of these mutations significantly affects growth or RNA transport (31, 49, 50). Removal of the C-terminal p80 portion (as in the *nup145-10* allele) causes temperature-sensitive growth and RNA export defects similar to those seen in strains that lack *RAT2/NUP120* (1, 22), *RAT3/NUP133* (12, 30, 33), *RAT9/NUP85* (18), *NUP82* (20, 24), or the carboxyl-terminal portion of *RAT7/NUP159* (19). Thus, loss of all or part of several nucleoporins is compatible with growth and RNA export at 23°C, but both growth and RNA export are defective in mutant strains at elevated temperatures.

A question that remains concerns the importance of this proteolytic processing. The fact that mutations that prevent cleavage of Nup145p are viable may mean that the p65 and p80 polypeptides from Nup145p are normally sufficiently close within the NPC that they can continue to perform their functions even when fused. A second possibility is that the more
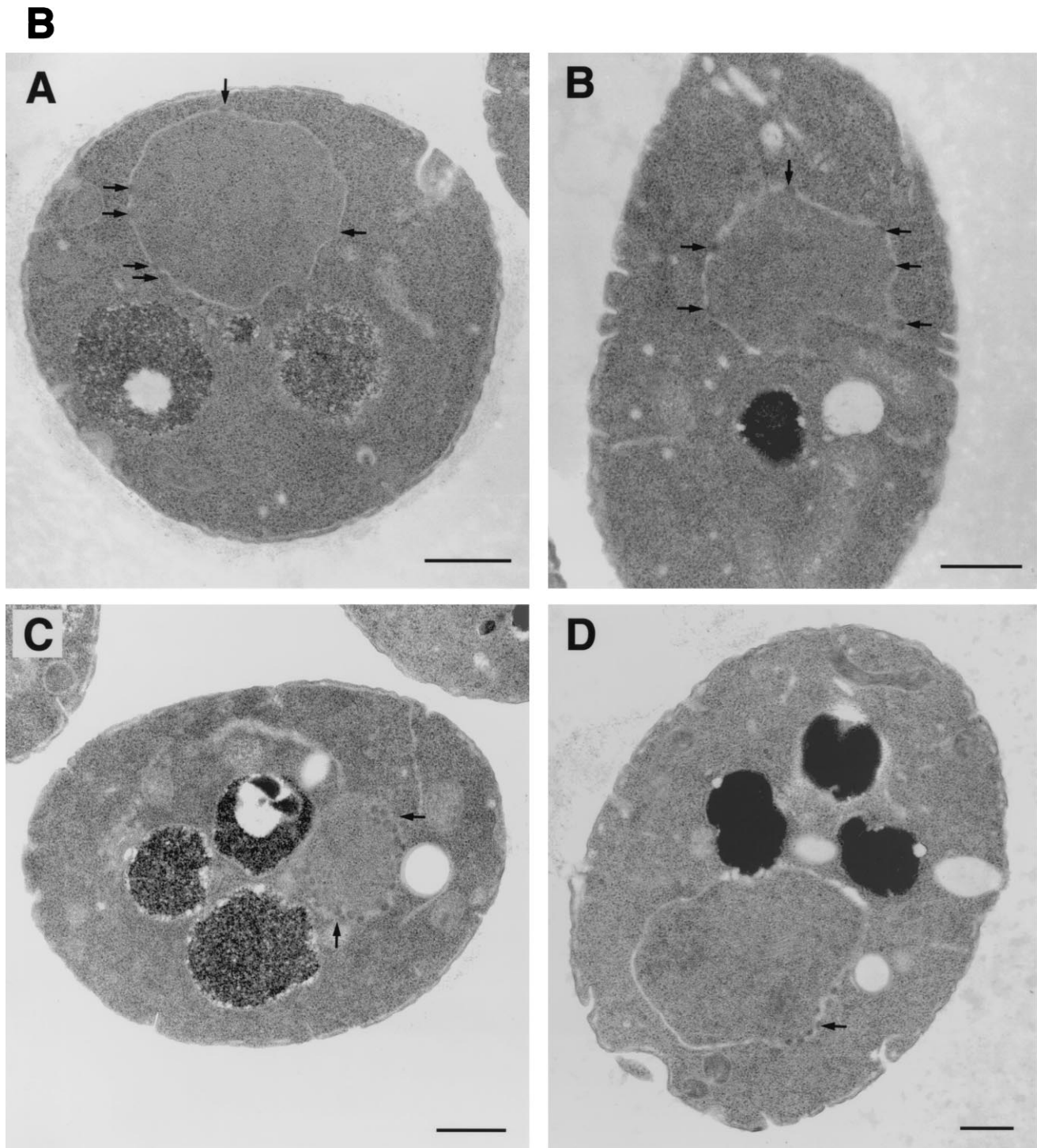
FIG. 7—*Continued.*

essential p80 polypeptide (required for RNA export at 37°C) may be capable of proper function even when the p65 polypeptide is linked to it. Our observation that a central deletion that blocks cleavage (*nup145-22*) does not result in significant defects in growth, morphology, or RNA export argues that both portions of Nup145p can perform their roles when fused. However, there may well be genetic backgrounds, for example, in

strains lacking part or all of specific nucleoporins, where the inability to cleave Nup145p is lethal.

While removal of no single domain of Nup145p grossly affected cell growth (references 14 and 47 and this study), deletion of the entire coding sequence produces cells that grow extremely poorly (Fig. 2). Removal of the entire gene product thus seems to produce defects similar to the synthetic lethal
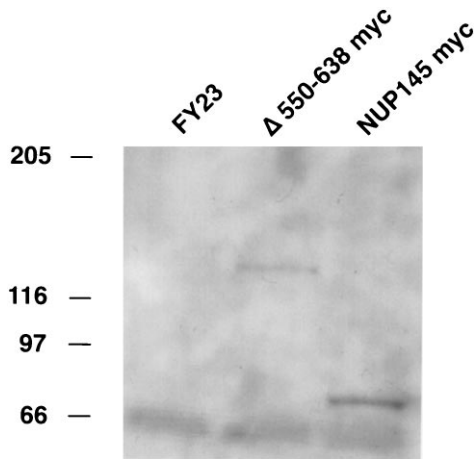
FIG. 8. Western analysis of cell extracts prepared from the strains containing epitope-tagged forms of wild-type Nup145p and the internal deletion mutant protein encoded by the *nup145-22* allele (CHY136; Δ550-638). Molecular masses (in kilodaltons) are indicated on the left.
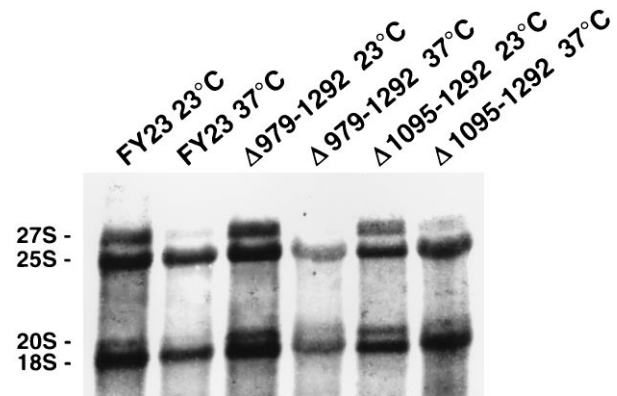


FIG. 9. rRNA processing in wild-type cells and *nup145* mutants at 23 and 37°C. Cells were labeled with [³H]uridine and processed as described in Materials and Methods. Lanes 1 and 2, wild-type cells; lanes 2 and 3, *nup145-13* cells (Δ979-1292); lanes 5 and 6, *nup145-14* (Δ1095-1292) cells.

phenotypes that have often been seen when cells carry null or defective alleles for two nucleoporins. We found that the *nup145-10* allele (essentially lacking the p80 portion) was synthetically lethal with the *rat7-1/nup159-1* and *rat3-1/nup133-1* mutations (10). Wente and Blobel (47) reported synthetic lethality between the mutation which eliminates the N-terminal portion of Nup145p and deletion of *NUP116* and observed both growth defects and enhanced morphological abnormalities when the Nup145p N-terminal mutation was combined with a disruption of *NUP100*. We expect that a lack of either the p65 or the p80 portion will result in synthetic lethality with a variety of other nucleoporin mutations.

**Ultrastructure defects with *NUP145* mutants.** Mutations of the C-terminal region of Nup145p produce defects in growth and/or nuclear structure. Deletions of amino acids between 698 and 979 lead to NPC clustering, while a deletion from amino acids 1095 to 1292 produced a milder clustering phenotype. Defects in nuclear shape were observed in cells carrying the *nup145-10* allele, as evaluated by electron microscopy (Fig. 4B). NPC clustering has been observed in yeast cells harboring various nucleoporin mutations (12, 18, 19, 22, 30, 47), yet this phenotype often imposes only moderate constraints on growth. Misshapen nuclei have been reported with the *nup1-106* mutation (6) and an allele of *NUP85* (18). It is not clear how such ultrastructural defects arise in strains lacking individual nucleoporins or containing defective nucleoporins. Disruption of interactions between NPCs and nuclear or cytoplasmic structures has been proposed as a mechanism by which NPCs could aggregate (12, 19, 47). It is also possible that even at permissive growth temperatures, nucleocytoplasmic exchange is reduced and that various components needed for production or maintenance of nuclear structure may not be present in adequate amounts.

Disruption of nucleolar structure was observed in the strains with all tested C-terminal mutations of Nup145p upon a shift to 37°C, including those that were not temperature sensitive for growth. The changes in nucleolar structure were correlated with decreases in the incorporation of [³H]uridine into RNA of 75% or greater, but rRNA processing remained quite normal (Fig. 9). The basis for the defects in nucleolar structure is not known, but the phenotype is consistently linked with defects in nucleocytoplasmic trafficking, as a variety of yeast mutants defective in RNA export show such a phenotype (1, 18, 22, 29,

42), as do mutants of the nuclear localization signal-binding protein Srp1p (54). As has been hypothesized for other nuclear structure defects, it may be possible that the nucleolus is sensitive to imbalances in the biosynthesis of components necessary to maintain its structure and/or function and that even mild perturbations of RNA export or nuclear protein import may result in alterations to nucleolar structure.

**Nup145p and RNA export.** Nup145p has previously been implicated in poly(A)⁺ RNA trafficking. Fabre et al. (14) found that an NRM in Nup145p centered around amino acid 489 binds RNA homopolymers in vitro. Similar motifs were also found in the nucleoporins Nup100p and Nup116p. Deletion of the NRM from Nup145p was found to have no significant effect upon cell growth, but deletion of the motif from Nup145p and Nup116p in a strain carrying a complete disruption of *NUP100* did render cells temperature sensitive. Depletion of Nup145p via repression of its expression from a glucose-repressible promoter results in nuclear poly(A)⁺ RNA accumulation in approximately 30% of the cells 3 h after transcription of *NUP145* was repressed and in nearly all cells 12 h after down-regulation (14). A deletion of *NUP116* coupled with a depletion of Nup145p accelerates the rate at which defects in poly(A)⁺ RNA become pronounced. These results prompted a hypothesis that RNA trafficking may be a primary function of Nup145p (14). The depletion study described above has the disadvantage of not allowing one to address which domain of Nup145p was affecting nucleocytoplasmic trafficking. Nuclear accumulation of poly(A)⁺ RNA has not been observed in yeast strain SWY77, a strain that fails to express the N-terminal 550 amino acids of Nup145p (10, 47). These results suggest that multiple domains of Nup145p (e.g., the p80 portion and the NRM) may be involved in RNA export functions of Nup145p.

In this study, we show that poly(A)⁺ RNA trafficking defects that are observed with Nup145p mutations are due to mutations in the C-terminal domain of the Nup145p peptide, with the strength of the nuclear accumulation being dependent upon the extent of truncation from the C terminus (Fig. 1B). While the C-terminal truncations of Nup145p affected poly(A)⁺ RNA trafficking, they did not have a notable effect on rRNA processing (Fig. 9). This is of interest because processing of the 20S precursor to the 18S mature form is believed to occur in the cytoplasm in yeast (46); thus, comparison of the ratios of 18 to 20S rRNA species can give an indication of the efficiency of rRNA export from the nucleus. Studies utilizing

injections of labeled RNA species into *Xenopus* oocytes have suggested that there are both common and specific factors that influence export of various RNA species (26). Nucleocytoplasmic shuttling of importin-α and of hnRNP A1 appears to occur via different pathways (34). Whether specific components of the NPC have differing affinities for importin-α and hnRNP A1 remains to be seen. It may be that the C-terminal domain of Nup145p is part of a complex that has specificity for export of poly(A)$^+$ RNA and not rRNA.

**What is the essential function of Nup145p?** Mutations of *NUP145* lead to a variety of defects. The NPC clustering and nuclear structure defects seen in cells with mutant alleles of *NUP145* suggest that parts of the protein play a structural role, as has been proposed for other nucleoporins that produce such a phenotype upon mutation. A role for Nup145p in RNA trafficking is suggested as well, based upon results presented here and results of Fabre et al. (14).

The multiple protein-protein interactions present in NPCs raise the possibility that mutant forms of individual nucleoporins may have weakened interactions with other surrounding nucleoporins. In the case of temperature-sensitive mutants, a change to the nonpermissive temperature may be sufficient to disrupt such interactions, possibly causing a loss of the mutant nucleoporin or other nucleoporins as well from the NPC. Nucleoporins that are nonessential for viability may not be incorporated into the NPC when mutated. Loss of nucleoporins from the NPC has been observed with mutant alleles of *NUP159*, *NUP82*, and *NUP85* (18, 19, 24). These possibilities make it difficult to ascribe a specific function to a nucleoporin through the use of depletion studies or temperature-sensitive mutants. In this light, it is interesting that non-temperature-sensitive alleles of *NUP145* examined in this study do show at least modest poly(A)$^+$ RNA trafficking defects. Elucidation of specific roles for nucleoporins in nucleocytoplasmic trafficking will also require that transport substrates that may contact the surface of the NPC channel be identified and that interaction with a specific nucleoporin in question be demonstrated.

Mutation of *NUP145* can lead to at least three phenotypes: conditional poly(A)$^+$ RNA export and nucleolar fragmentation defects resulting from a C-terminal truncation and NPC clustering resulting from either N-terminal or C-terminal deletions. Most likely, the C-terminal domain of Nup145p is a component of a substructure within the yeast NPC that has roles in maintaining NPC distribution and poly(A)$^+$ RNA trafficking.

## REFERENCES

1. **Aitchison, J. D., G. Blobel, and M. P. Rout.** 1995. Nup120p: a yeast nucleoporin required for NPC distribution and mRNA transport. J. Cell Biol. **131:**1659–1675.
2. **Akey, C. W., and M. Radermacher.** 1993. Architecture of the Xenopus nuclear pore complex revealed by three-dimensional cryo-electron microscopy. J. Cell Biol. **122:**1–19.
3. **Amberg, D. A., A. L. Goldstein, and C. N. Cole.** 1992. Isolation and characterization of *RAT1*, an essential gene of *Saccharomyces cerevisiae* required for the efficient nucleocytoplasmic trafficking of mRNA. Genes Dev. **6:**1173–1189.
4. **Aris, J. P., and G. Blobel.** 1988. Identification and characterization of a yeast nucleolar protein that is similar to a rat liver nucleolar protein. J. Cell Biol. **107:**17–31.
5. **Baudin, A., O. Ozier-Kalogeropoulos, A. Denouel, F. Lacroute, and C. Cullin.** 1993. A simple and efficient method for direct gene deletion in *Saccharomyces cerevisiae*. Nucleic Acids Res. **21:**3329–3330.
6. **Bogerd, A. M., J. A. Hoffman, D. C. Amberg, G. R. Fink, and L. I. Davis.** 1994. *nup1* mutants exhibit pleiotropic defects in nuclear pore complex function. J. Cell Biol. **127:**319–332.
7. **Byers, B., and L. Goetsch.** 1975. Behavior of spindles and spindle plaques in the cell cycle and conjugation of *Saccharomyces cerevisiae*. J. Bacteriol. **124:**511–523.
8. **Copeland, C. S., and M. Snyder.** 1993. Nuclear pore complex antigens delineate nuclear envelope dynamics in vegetative and conjugating *Saccharomyces cerevisiae*. Yeast **9:**235–249.
9. **Davis, L. I.** 1995. The nuclear pore complex. Annu. Rev. Biochem. **64:**865–896.
10. **Dockendorff, T. C., and C. N. Cole.** Unpublished data.
11. **Doye, V., and E. C. Hurt.** 1995. Genetic approaches to nuclear pore structure and function. Trends Genet. **11:**235–241.
12. **Doye, V., R. Wepf, and E. C. Hurt.** 1994. A novel nuclear pore protein Nup133p with distinct roles in poly(A)$^+$ RNA transport and nuclear pore distribution. EMBO J. **13:**6062–6075.
13. **Elliot, D. J., F. Stutz, A. Lescure, and M. Rosbash.** 1994. mRNA nuclear transport. Curr. Opin. Genet. Dev. **4:**305–309.
14. **Fabre, E., W. C. Boelens, C. Wimmer, I. W. Mattaj, and E. C. Hurt.** 1994. Nup145p is required for nuclear export of mRNA and binds homopolymeric RNA in vitro via a novel conserved motif. Cell **78:**275–289.
15. **Fabre, E., and E. C. Hurt.** 1994. Nuclear transport. Curr. Opin. Cell Biol. **6:**335–342.
16. **Gietz, R. D., and A. Sugino.** 1988. New yeast-*Escherichia coli* shuttle vectors constructed with *in vitro* mutagenized yeast genes lacking six-base pair restriction sites. Gene **74:**527–534.
17. **Goldberg, M. W., and T. D. Allen.** 1992. High resolution scanning electron microscopy of the nuclear envelope: the baskets of the nucleoplasmic face of the nuclear pores. J. Cell Biol. **119:**1429–1440.
18. **Goldstein, A. L., C. A. Snay, C. V. Heath, and C. N. Cole.** 1996. Pleiotropic nuclear defects associated with a conditional allele of the novel nucleoporin Rat9p/Nup85p. Mol. Biol. Cell **7:**917–934.
19. **Gorsch, L. C., T. C. Dockendorff, and C. N. Cole.** 1995. A conditional allele of the novel repeat-containing yeast nucleoporin *RAT7/NUP159* causes both rapid cessation of mRNA export and reversible clustering of nuclear pore complexes. J. Cell Biol. **129:**939–955.
20. **Grandi, P., S. Emig, C. Weise, F. Hucho, T. Pohl, and E. C. Hurt.** 1995. A novel nuclear pore protein Nup82p which specifically binds to a fraction of Nsp1p. J. Cell Biol. **130:**1263–1273.
21. **Guthrie, C., and G. R. Fink.** 1991. Guide to yeast genetics and molecular biology. Methods Enzymol. **194:**423–424.
22. **Heath, C. V., C. S. Copeland, D. C. Amberg, V. Del Priore, M. Snyder, and C. N. Cole.** 1995. Nuclear pore complex clustering and nuclear accumulation of poly(A)$^+$ RNA associated with mutations of the *Saccharomyces cerevisiae RAT2/NUP120* gene. J. Cell Biol. **131:**1677–1697.
23. **Hinshaw, J. E., B. O. Carragher, and R. A. Milligan.** 1992. Architecture and design of the nuclear pore complex. Cell **69:**1133–1141.
24. **Hurwitz, M. E., and G. Blobel.** 1995. NUP82 is an essential yeast nucleoporin required for poly(A)$^+$ RNA export. J. Cell Biol. **130:**1275–1281.
25. **Izaurralde, E., and I. W. Mattaj.** 1995. RNA export. Cell **81:**153–159.
26. **Jarmolowski, A., W. C. Boelens, E. Izaurralde, and I. W. Mattaj.** 1994. Nuclear export of different classes of RNA is mediated by specific factors. J. Cell Biol. **124:**627–635.
27. **Jarnik, M., and U. Aebi.** 1991. Toward a more complete 3-D structure of the nuclear pore complex. J. Struct. Biol. **107:**291–308.
28. **Jones, J. S., and L. Prakash.** 1990. Yeast *Saccharomyces cerevisiae* selectable markers in pUC18 polylinkers. Yeast **6:**363–366.
29. **Kadowaki, T., R. Schneiter, M. Hitomi, and A. M. Tartakoff.** 1995. Mutations in nucleolar proteins lead to nucleolar accumulation of poly(A)$^+$ RNA in *Saccharomyces cerevisiae*. Mol. Biol. Cell **6:**1103–1110.
30. **Li, O., C. V. Heath, D. C. Amberg, T. C. Dockendorff, C. S. Copeland, M. Snyder, and C. N. Cole.** 1995. Mutation or deletion of the *Saccharomyces cerevisiae RAT3/NUP133* gene causes temperature-dependent nuclear accumulation of poly(A)$^+$ RNA and constitutive clustering of nuclear pore complexes. Mol. Biol. Cell **6:**401–417.
31. **Loeb, J., L. I. Davis, and G. R. Fink.** 1993. NUP2, a novel yeast nucleoporin, has functional overlap with other proteins of the nuclear pore complex. Mol. Biol. Cell **4:**209–222.
32. **Nehrbass, U., H. Kern, A. Mutvei, H. Horstmann, B. Marshallsay, and E. C. Hurt.** 1990. NSP1: a yeast nuclear envelope protein localized at the nuclear pores exerts its essential function by its carboxy-terminal domain. Cell **61:**979–989.
33. **Pemberton, L. F., M. P. Rout, and G. Blobel.** 1995. Disruption of the nucleoporin gene NUP133 results in clustering of nuclear pore complexes. Proc. Natl. Acad. Sci. USA **92:**1187–1191.
34. **Pollard, V. W., W. M. Michael, S. Nakielny, M. Siomi, F. Wang, and G.**

**Dreyfuss.** 1996. A novel receptor-mediated nuclear protein import pathway. Cell **86:**985–994.

35. **Ris, H.** 1991. The three-dimensional structure of the nuclear pore complex as seen by high voltage electron microscopy and high resolution low voltage scanning electron microscopy. EMSA Bull. **21:**54–56.
36. **Rose, M. D., P. Novick, J. H. Thomas, D. Botstein, and G. R. Fink.** 1987. A *Saccharomyces cerevisiae* genomic plasmid bank based on a centromere-containing shuttle vector. Gene **60:**237–243.
37. **Rose, M. D., F. Winston, and P. Hieter.** 1989. Methods in yeast genetics. Cold Spring Harbor Laboratory Press, Cold Spring Harbor, N.Y.
38. **Rothstein, R.** 1991. Targeting, disruption, replacement, and allele rescue: integrative DNA transformation in yeast. Methods Enzymol. **194:**281–301.
39. **Rout, M. P., and G. Blobel.** 1993. Isolation of the yeast nuclear pore complex. J. Cell Biol. **123:**771–783.
40. **Rout, M. P., and S. R. Wente.** 1994. Pores for thought: nuclear pore complex proteins. Trends Cell Biol. **4:**357–365.
41. **Sambrook, J., E. F. Fritsch, and T. Maniatis.** 1989. Molecular cloning: a laboratory manual, 2nd ed. Cold Spring Harbor Laboratory Press, Cold Spring Harbor, N.Y.
42. **Schneiter, R., T. Kadowaki, and A. M. Tartakoff.** 1995. mRNA transport in yeast: time to reinvestigate the functions of the nucleolus. Mol. Biol. Cell **6:**357–370.
43. **Sherman, F.** 1991. Getting started with yeast. Methods Enzymol. **194:**3–21.
44. **Snow, C. M., A. Senior, and L. Gerace.** 1987. Monoclonal antibodies identify a group of nuclear pore complex glycoproteins. J. Cell Biol. **104:**1143–1156.
45. **Spurr, A. R.** 1969. A low-viscosity resin embedding medium for electron microscopy. J. Ultrastruct. Res. **26:**31–43.
46. **Udem, S. A., and J. R. Warner.** 1973. The cytoplasmic maturation of a ribosomal precursor RNA in yeast. J. Biol. Chem. **248:**1412–1416.
47. **Wente, S. R., and G. Blobel.** 1994. *NUP145* encodes a novel yeast glycine-leucine-phenylalanine-glycine (GLFG) nucleoporin required for nuclear envelope structure. J. Cell Biol. **125:**955–969.
48. **Wente, S. R., and G. Blobel.** 1993. A temperature-sensitive NUP116 null mutant forms a nuclear envelope seal over the yeast nuclear pore complex, thereby blocking nucleocytoplasmic traffic. J. Cell Biol. **123:**275–284.
49. **Wente, S. R., M. P. Rout, and G. Blobel.** 1992. A new family of yeast nuclear pore complex proteins. J. Cell Biol. **119:**705–723.
50. **Wimmer, C., V. Doye, P. Grandi, U. Nehrbass, and E. C. Hurt.** 1992. A new subclass of nucleoporins that functionally interact with nuclear pore protein NSP1. EMBO J. **11:**5051–5061.
51. **Winston, F., C. Dollard, and S. L. Ricupero-Hovasse.** 1995. Construction of a set of convenient *Saccharomyces cerevisiae* strains that are isogenic to S288C. Yeast **11:**53–55.
52. **Woolford, J. L., Jr., and J. R. Warner.** 1991. The ribosome and its synthesis, p. 587–626. *In* J. R. Broach, J. R. Pringle, and E. W. Jones (ed.), The molecular and cellular biology of the yeast *Saccharomyces*: genome dynamics, protein synthesis and energetics. Cold Spring Harbor Laboratory Press, Cold Spring Harbor, N.Y.
53. **Wright, R., and J. Rine.** 1989. Transmission electron microscopy and immunocytochemical studies of yeast: analysis of HMG-CoA reductase overproduction by electron microscopy. Methods Cell Biol. **31:**473–512.
54. **Yano, R., M. L. Oakes, M. M. Tabb, and M. Nomura.** 1994. Yeast Srp1p has homology to armadillo/plakoglobin/β-catenin and participates in apparently multiple nuclear functions including the maintenance of nucleolar structure. Proc. Natl. Acad. Sci. USA **91:**6880–6884.